Optimization of OFDM Parameters for 10-Gbps Long Reach Coherent PONs

Antonio Ferreira[1], Bruna Dias[1], Jose Augusto de Oliveira[1], Andre Alves[1], Jorge D. Marconi[2], Gabriel Campuzano[3], Julian Pita[4], and Ivan Aldaya[1]

[1]*Campus São João da Boa Vista, State University of São Paulo, São Paulo, Brazil*

[2]*CEM, Universidade Federal do ABC, São Paulo, Brazil*

[3]*Department of Electrical and Computer Engineering, Tecnológico de Monterrey, Mexico*

[4]*FEEC, Universidade Estadual de Campinas, Campinas, Brazil*

e-mail: antonio.elcio@unesp.br, ivan.a.aldaya@ieee.org

ABSTRACT

Coherent passive optical networks (PONs) employing orthogonal frequency division modulation (OFDM) have emerged as a promising candidate for the implementation of future long-reach high-capacity optical access infrastructure. In addition to the improved receiver sensitivity, coherent systems allow advanced vectorial modulation formats and, thus, make a more efficient use of the spectrum. Mitigation of the phase noise, however, is still a challenge that must be addressed in low-cost access systems. In OFDM systems, in particular, pilot-aided equalization can be employed to efficiently combat this impairment. In this work, we present extensive simulation results to optimize a 100-km LR-PON with 10-Gbps capacity in terms of the number of subcarriers and pilots, as well as the relative power of the pilots. These results reveal that 64 subcarriers, being 10 of them pilots, and a relative amplitude of 1.8 leads to a BER of 4.736×10^{-4}.

1. INTRODUCTION

In order to meet the increasing capacity demand, network operators are progressively extending their optical fibers closer to end users [1], [2]. Passive optical networks (PONs), which has proven to offer cost-effective broadband data transmission for up to 20 km, are then required to achieve longer ranges. Thus, 100 km is usually considered as the target for future long-reach (LR)-PONs [3]-[6]. The longer distance leads to higher attenuation, which further requires a deep modification of the traditional PON architecture. One of the proposed solution is the use of active amplifying nodes [3], [4]. This approach, even if effective, makes the complex distribution more complex and increases the operational cost and power consumption. An alternative solution relays on coherent detection [6]. It is well-known that due to the mixing with a strong local oscillator, receivers based on homodyne detection enjoy an improved sensitivity [7], [8]. In addition, coherent systems allows vectorial modulations that, when detected, occupy half the bandwidth of that using direct detection, which further contributes to enhance the receiver sensitivity [8]. Coherent systems, however, present two challenges that lead to amplitude variation of the photodetected signals [9]: (i) polarization mismatch between the received signal and local oscillator and (ii) the lack of phase correlation of the oscillators employed in the transmitter and receiver. Since the coherence time of the state-of-polarization is significantly longer than that of the combined phase noise (considering the random phases of both oscillators), the compensation of phase noise is critical. In LR-PONs, particularly, the stringent cost requirements make the use of narrow-linewidth laser prohibitively expensive, which results in a phase noise significantly higher than in long-haul multi-span coherent systems.

In regards to the modulation format, orthogonal frequency division multiplexing (OFDM) has attracted an increasing attention for LR-PONs [3]-[6]. This format has already been chosen for intensity-modulated direct detection PON systems [10], [11]. For instance, the NGPON2 standard that will govern the implementation of the second stage of next generation PONs, employs OFDM because of its high spectral efficiency and service granularity. In addition, given the multi-carrier nature, OFDM is robust against chromatic dispersion and other frequency selective impairments [12], [13]. Phase noise, on the other hand, is responsible for breaking the orthogonality among the subcarriers, resulting in common phase error (CPE) and inter-carrier interference (ICI) [14], [15]. There are two commonly adopted strategies to mitigate for phase noise in OFDM optical systems [16], namely, data-aided and pilot-aided phase synchronization. The former results in higher spectral efficiency but it is subject to phase ambiguity and cannot compensate for additional frequency selective impairments, hence, in OFDM systems the latter is preferable. Pilot-aided equalization, however, is capable to compensate only the CPE and not ICI, whose relative impact strongly depends on OFDM signal parameters, especially on the subcarrier frequency separation (which is the inverse of the OFDM period) [14]. Thus, phase noise is mitigated more efficiently for short OFDM symbols (typically low number of subcarriers), where the relative power of ICI is small compared to that of CPE [15]. The number of pilots and their relative amplitude with respect to data subcarriers, on the other hand, are critical in the channel equalization and, consequently, in the overall system performance. A high number of strong pilots will lead to robustness against additive noise but, in case of an excessively large number of pilots, the signal will be more sensitive to nonlinear effects and the spectral efficiency will be reduced. Given the complex interplay between signal parameters and physical impairments, the setup of OFDM parameters is not trivial, since it is necessary to accounts for parameters such as pilot amplitudes, number of subcarriers and pilots, and driving amplitude. In this work we present the results of

extensive simulations to simultaneously optimize the number of data and pilot subcarriers, as well as their relative amplitude in a 10-Gbps coherent PON with up to 100-km range and a splitting ratio of 64 users. Results reveal that a bit error rate (BER) of less than 10^{-3} can be achieved using either 32, or 64 subcarriers but the optimum BER is obtained for 64 subcarriers from which 10 subcarriers are used for pilots with a relative amplitude of 1.8 lead to optimal performance (BER $\sim 4.736\times10^{-4}$).

2. SIMULATION SETUP

Figure 1(a) shows the simulation setup employed to analyze the system performance of the different OFDM configurations. The system under test was evaluated using Matlab/VPI Transmission Maker co-simulation where the OFDM modulation and demodulation were implemented in Matlab and the electrical-to-optical conversion, fiber transmission, and signal detection were simulated in VPI Transmission Maker. In the OFDM modulator, a pseudorandom sequence was parallelized in blocks of N_b bits and mapped into a quadrature phase shift keying (QPSK) constellation [Fig. 1(b)], resulting in $N_{data} = N_b/2$ data subcarriers. After uniformly interleaving N_p pilots [Fig. 1(c)], the Inverse Fast Fourier Transform (IFFT) of $N_{SC} = N_p + N_{data}$ points was computed and a cyclic prefix (CP) of 10% of the symbol period was added. The resulting block was serialized and decomposed into its real [whose spectrum is shown in Fig. 1(d)] and imaginary parts, which were oversampled and interpolated using a 3rd order polynomial to emulate the digital to analog conversion (DAC). The two real-valued signals corresponding to the in-phase and quadrature components drove the RF inputs of a dual-parallel Mach-Zehnder modulator (DP-MZM) that modulated the output of a continuous wave (CW) laser diode (LD1) operating at 1550 nm. The output of the DP-MZM was amplified before being transmitted over an 80-km standard single mode fiber (SSMF) span [Fig. 1(e)]. The signal was then attenuated 20 dB to account for splitting losses (64 users and insertion loss) and transmitted through a second SSMF span of 20 km. At the receiver side, the incoming signal was combined with a second CW laser (LD2) using a 90° hybrid network. The four outputs were detected employing two pairs of balanced photodetectors (PDs), resulting in two differential signals [Fig. 1(f)] that were demodulated by performing the inverse steps of the modulator, that is, downsampling, removal of CP, computation of the Fast Fourier Transform (FFT), pilot-aided equalization using linear interpolation, and QPSK demapping. The constellations before and after pilot-aided equalization are shown in Fig. 1(g) and (h), respectively. The system performance for the different OFDM configurations was assessed by comparing the generated and demodulated bit sequences and computing the BER by error counting. All the simulations considered a bit rate of 10 Gbps and a simulation window of 6553.6 ns but, since the OFDM symbol period may differ for different configurations, the number of OFDM and, therefore, bits, is not the same for all the cases (the number of simulated bits ranges from 65314 to 65516). Table 1 summarizes the simulation parameters.

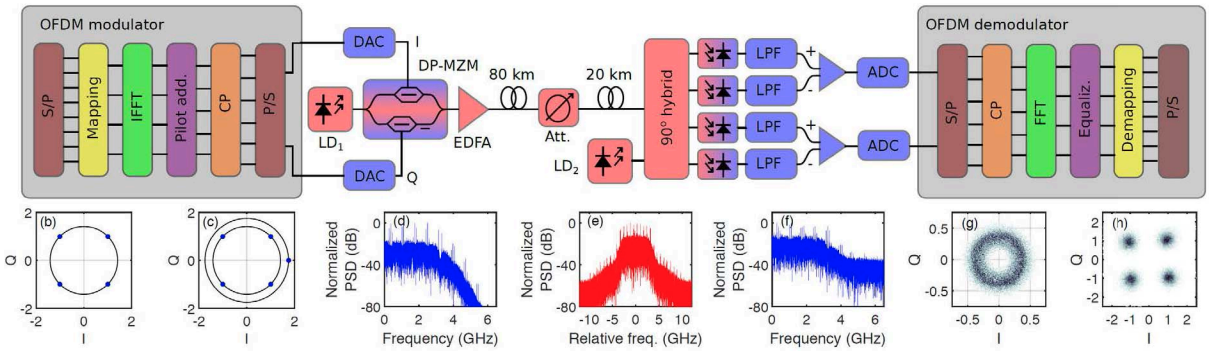

Figure 1: (a) Block diagram of the simulated system. S/P: serial-to-parallel conversion. IFFT: Inverse Fast Fourier Transform. CP: cyclic prefix addition. P/S: parallel-to-serial conversion. DAC: digital to analog converter. LD: laser diode. DP-MZM: dual parallel-Mach-Zehnder modulator. EDFA: erbium-doped fiber amplifier. Att: attenuator. PD: photodetector. LPF: low-pass filter. ADC: analog-to-digital converter. FFT: Fast Fourier Transform. Constellation diagrams (b) before and (c) after pilot inclusion, (d) spectrum of the generated in-phase electrical signal, (e) optical spectrum, (f) photogenerated in-phase signal, (g) constellation before pilot-aided equalization, and (h) constellation after equalization.

Table 1. Parameters used in the simulation.

System parameters			
Laser linewidth	1 MHz	Fiber length	80 km, 20 km
Laser power	10 mW	Fiber attenuation	0.2 dB
MZM insertion loss	6 dB	Fiber chromatic dispersion	16 ps/nm/km
Amplifier gain	20 dB	Fiber PMD	3.16×10^{-15} s/km$^{1/2}$
Amplifier noise figure	4 dB	Nonlinear coefficient	2.6×10^{-20} m^2 /W
Attenuator	20 dB	Fiber effective area	80 µm^2
PD thermal noise density	10 pA/Hz$^{1/2}$	Electrical filter bandwidth	5 GHz
PD responsivity	1 W/A	Electrical filter order	4

Signal parameters	
Number of subcarriers	32, 64, 128
Number of pilots	3, 5, 10, 15, 20, 25
Subcarrier modulation format	QPSK
Cyclic prefix duration	10%
Bit rate	10 Gbps
Simulation parameters	
Time window	6553.6 ns
Sampling rate	160×10^9 s^{-1}

3. RESULTS AND DISCUSSION

The simulation results considering different numbers of pilots, subcarriers, and amplitude ratios are shown in Fig. 2. The contour plots presented in Fig. 2(a-c) represent the obtained BER for 32 subcarriers and 3, 5, and 10 pilots, respectively, in terms of the pilot-to-data subcarrier amplitude ratio and the root mean squared (rms) driving amplitude normalized to the π voltage of the modulator (V_π = 5 V). In all the three cases, extreme values of driving amplitude result in degraded BER. On the one hand, when driving amplitude is low, the power of the modulated signal is weak and, consequently, the signal-to-noise (SNR) is poor. For high driving amplitudes, on the other hand, the nonlinear distortion, dominated by the MZM response, degrades the signal. A similar behavior occurs when the relative amplitude of the pilots is varied. If their amplitude is low, the interpolation process is strongly affected by the receiver noise, whereas if their amplitude is high, the signal presents a high

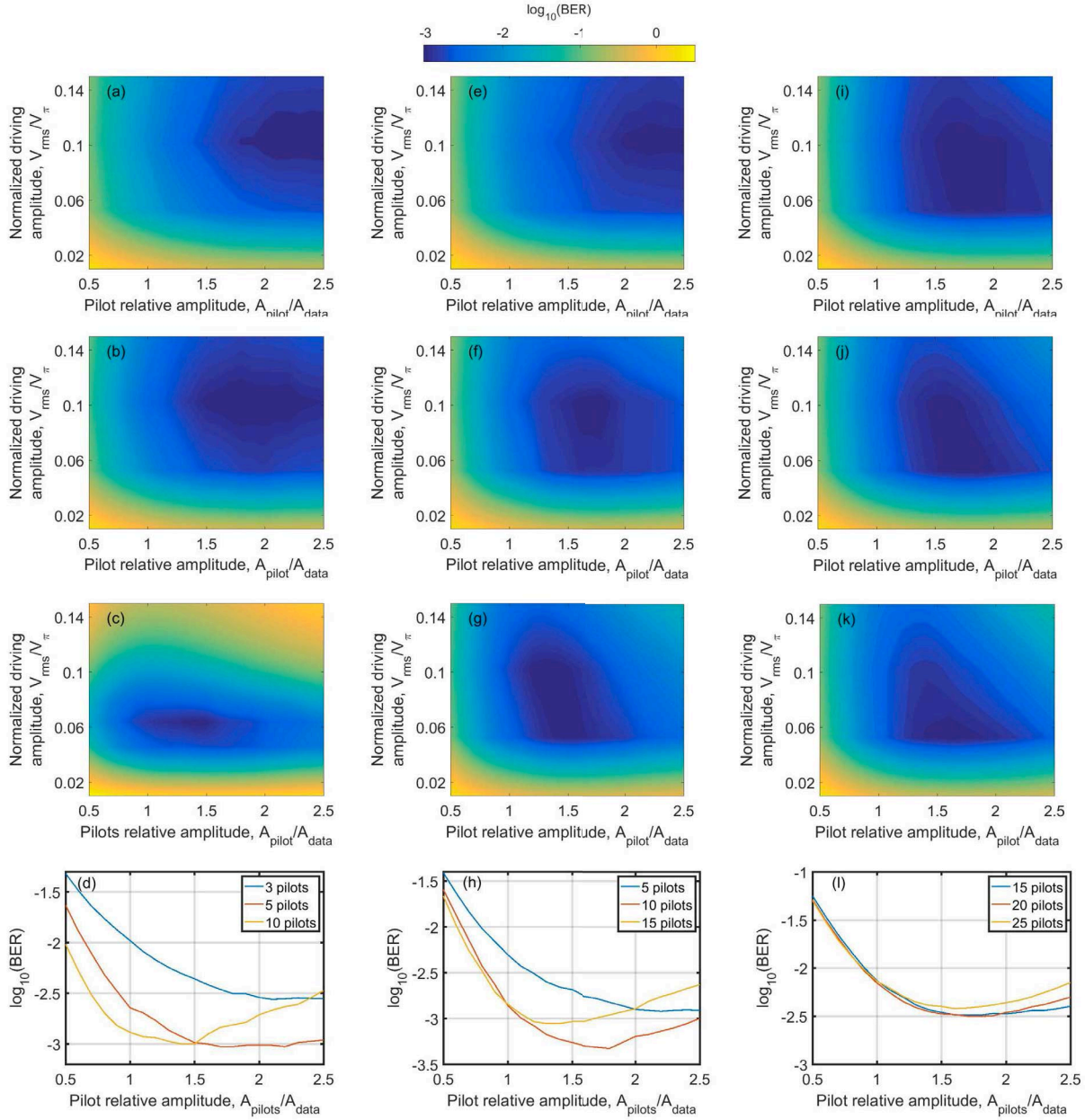

Figure 2. Simulation results for different OFDM signal configurations. (a-c) Contour plots showing the obtained BER in terms of the relative pilot amplitude and driving amplitude for 32 subcarriers and 3, 5 and 10 pilots. (d) BER as a function of the relative pilot amplitude at optimum driving amplitudes. (e-g) and (h) are equivalent to (a-c) and (d) but for 64 subcarriers and 5, 10, and 15 pilots, whereas (i-k) and (l) are for 128 subcarriers with 15, 20, and 25 pilots.

Table 2. Summary of optimum performance configurations.

Signal parameters					
Number of subcarriers	Number of pilots	Relative pilot amplitude A_{pilot}/A_{data}	Norm. amplitude V_{rms}/V_π	Simulated bits	BER
32	5	1.7	0.1025	65502	9.473×10^{-4}
64	10	1.8	0.1025	65448	4.736×10^{-4}
128	20	1.8	0.1025	65448	3.178×10^{-3}

peak-to-average power ratio, becoming it very sensitive to nonlinear distortion. From these contour plots, the BER value for each relative pilot amplitude at optimum driving amplitude is obtained and presented in Fig. 2(d). For the three considered amounts of pilots, it can be seen that the optimum relative amplitude depends on the number of employed pilot subcarriers. Thus, the larger the number of pilots is, the lower the optimum relative amplitude results. This can be explained by noting that for a higher number of pilots, the equalization is more robust to noise and, hence a lower pilot amplitude can be employed. For a lower number of pilots, on the contrary, higher power is required, even if this results in stronger nonlinear distortion. It is worth noting that for the three cases, the pilots should have higher amplitude than data subcarriers. Indeed, for this number of subcarriers, when comparing the BER with optimum amplitude to unity amplitude ratio, we see that we have an improvement from 0.01 to 2.8×10^{-3} for 3 pilots, from 2.5×10^{-3} to 9.4×10^{-4} for 5 and from 1.3×10^{-3} to 1.0×10^{-3} for 15 pilots. Fig. 2(e-g) and 2(h) are similar to Fig. 2(a-c) and (d) but for 64 subcarriers, showing a similar behavior. Finally, Fig. 2(i-k) and 2(l) are for 128 subcarriers. It can be seen that, independently of the number of subcarriers, the trade-off between noise and nonlinear distortion persists.

Table 2 summarizes the best configurations for 32, 64 and 128 subcarriers, showing that the number of optimum pilots increases with the number of subcarriers but that the relative number of pilots was constant (around 16%). As mentioned before, in all the three cases the optimum BER was obtained for pilots having higher amplitude than data subcarriers. Comparing the system performance in terms of the number of subcarriers, it can be seen that the optimum value is achieved for 64 subcarriers (BER = 4.7×10^{-4}). For a higher number of subcarriers, the chromatic dispersion is a priori better compensated but, at the same time, the PAPR increases, resulting in a poorer performance.

4. CONCLUSIONS

In this work we optimized the signal parameters of coherent OFDM LR-PON. We employed a Matlab/VPI Transmission Maker co-simulation environment to assess the effect of the main OFDM parameters, revealing that the optimum performance is achieved for 64 subcarriers and 10 pilots with a relative amplitude of 1.8. In addition, we numerically confirmed the relation between the BER and the number of pilots and we show the importance of optimizing the relative amplitude of pilots to achieve optimum performance.

ACKNOWLEDGMENTS

Authors thank the São Paulo Research Foundation (FAPESP) (Proc. 2017/19557-6); the Conselho Nacional de Desenvolvimento Científico e Tecnológico (CNPq) (574017/2008-9); and the Coordination for the Improvement of Higher Education Personnel (CAPES).

REFERENCES

[1] D. Nesset, “PON roadmap,” *IEEE/OSA Journal of Optical Communications and Networking*, vol. 9, no. 1, pp. A71-A76, 2017.
[2] F. J. Effenberger, “Industrial trends and roadmap of access,” *Journal of Lightwave Technology*, vol. 35, no. 5, pp. 1142-1146, 2017.
[3] D.-Z. Hsu, C.-C. Wei, H.-Y. Chen, J. Chen, M. C. Yuang, S.-H. Lin, and W.-Y. Li, “21 Gb/s after 100 km OFDM long-reach PON transmission using a cost-effective electro-absorption modulator,” *Optics Express*, vol. 18, no. 26, pp. 27758-27763, 2010.
[4] M. Chen, J. He, and L. Chen, “Real-time optical OFDM long-reach PON system over 100 km SSMF using a directly modulated DFB laser,” *Journal of Optical Communications and Networking*, vol. 6, no. 1, pp. 18-25, 2014.
[5] D. Lavery, M. Ionescu, S. Makovejs, E. Torrengo, and S. J. Savory, “A long-reach ultra-dense 10 Gbit/s WDM-PON using a digital coherent receiver,” *Optics Express*, vol. 18, no. 25, pp. 25 855-25 860, 2010.
[6] D. Lavery, R. Maher, D. S. Millar, B. C. Thomsen, P. Bayvel, and S. J. Savory, “Digital coherent receivers for long-reach optical access networks,” *Journal of Lightwave Technology*, vol. 31, no. 4, pp. 609-620, 2013.
[7] G. P. Agrawal, *Fiber-Optic Communication Systems*. John Wiley & Sons, 2012, vol. 222.
[8] K. Kikuchi and S. Tsukamoto, “Evaluation of sensitivity of the digital coherent receiver,” *Journal of Lightwave Technology*, vol. 26, no. 13, pp. 1817-1822, 2008.
[9] K. Kikuchi, “Fundamentals of coherent optical fiber communications,” *Journal of Lightwave Technology*, vol. 34, no. 1, pp. 157-179, 2016.
[10] D. Nesset, “NG-PON2 technology and standards,” *Journal of Lightwave Technology*, vol. 33, no. 5, pp. 1136-1143, 2015.
[11] *Gigabit-Capable Passive Optical Networks (GPON): Enhancement Band*, ITU-T G.989 Series Recommendations, 2014. [12] W. Shieh and I. Djordjevic, *OFDM for Optical Communications*. Academic Press, 2009.
[13] J. Armstrong, “OFDM for optical communications,” *Journal of lightwave technology*, vol. 27, no. 3, pp. 189-204, 2009.
[14] A. Armada, “Understanding the effects of phase noise in orthogonal frequency division multiplexing,” *IEEE Transactions on Broadcasting*, vol. 47, no. 5, pp. 580-583, 1998.
[15] D. Zabala-Blanco, G. Campuzano, I. Aldaya, G. Castanon, and C. Vargas-Rosales, “Impact of partial phase decorrelation on the performance of pilot- assisted millimeter-wave RoF-OFDM systems,” *Physical Communication*, vol. 26, pp. 106-115, 2018.
[16] X. Yi, W. Shieh, and Y. Tang, “Phase estimation for coherent optical OFDM,” *IEEE Photonics Technology Letters*, vol. 19, no. 9/12, p. 919, 2007.